

Active foundering of a continental arc root beneath the southern Sierra Nevada in California

George Zandt¹, Hersh Gilbert¹, Thomas J. Owens², Mihai Ducea¹, Jason Saleeby³ & Craig H. Jones⁴

¹Department of Geosciences, University of Arizona, Tucson, Arizona 85721, USA

²Department of Geological Sciences, University of South Carolina, Chapel Hill, North Carolina 29208, USA

³Department of Geological and Planetary Sciences, California Institute of Technology, Pasadena, California 91125, USA

⁴Department of Geological Sciences, University of Colorado, Boulder, Colorado 80309, USA

Seismic data provide images of crust–mantle interactions during ongoing removal of the dense batholithic root beneath the southern Sierra Nevada mountains in California. The removal appears to have initiated between 10 and 3 Myr ago with a Rayleigh–Taylor-type instability, but with a pronounced asymmetric flow into a mantle downwelling (drip) beneath the adjacent Great Valley. A nearly horizontal shear zone accommodated the detachment of the ultramafic root from its granitoid batholith. With continuing flow into the mantle drip, viscous drag at the base of the remaining ~35-km-thick crust has thickened the crust by ~7 km in a narrow welt beneath the western flank of the range. Adjacent to the welt and at the top of the drip, a V-shaped cone of crust is being dragged down tens of kilometres into the core of the mantle drip, causing the disappearance of the Moho in the seismic images. Viscous coupling between the crust and mantle is therefore apparently driving present-day surface subsidence.

Giant magmatic bodies, or batholiths, that constitute nearly the entire crust in belts thousands of kilometres long are integral features of major mountain systems associated with continental arcs. There is a growing recognition that the growth of ~30-km-thick granitoid batholiths must involve a two-step magmatic differentiation process that generates an equal or even greater thickness of ultramafic residual roots beneath the granitic bodies (see, for example, ref. 1). Removal of such dense ultramafic roots is often cited as a mechanism for differentiation in Cordilleran arcs (see, for example, refs 2, 3) to produce the overall intermediate composition of the continents^{4,5}, but the actual timing and mechanism of removal, and whether all such roots eventually founder, remains uncertain. In southern California, a compelling case has been made for a late Cenozoic (<10 Myr ago) foundering event beneath the southern Sierra Nevada batholith^{6–10}. We present seismic results that provide direct evidence connecting crustal structures associated with the removal event to the mantle downwelling imaged in previous tomography studies^{11–13} (Supplementary Information). Analyses of receiver functions reveal seismic anisotropy at the base of the crust that may be related to shearing along a detachment zone that became a new crust–mantle boundary. Viscous drag at the base of the remaining ~35-km-thick crust has thickened it by ~7 km in a narrow crustal welt, and at the top of the drip, a V-shaped cone of crust is being dragged down tens of kilometres into the core of the mantle drip.

Crustal welts and missing Moho

A 20-station, PASSCAL experiment (in 1997) and five permanent stations in the TriNet network in this area recorded the teleseismic data used in this study (Fig. 1). The 25 stations encompass the southern Sierra Nevada region, where xenoliths from Miocene, Pliocene and Quaternary volcanic fields document the presence of an ultramafic root in the Miocene (~10 Myr ago) and its absence in the Pliocene (~3 Myr ago)^{6–8}. Residual garnet pyroxenite xenoliths found in mid-Miocene volcanic rocks from the Sierra Nevada⁶ are extremely dense rocks (3,500–3,600 kg m⁻³) compared with typical mantle peridotites (~3,300 kg m⁻³) owing to their garnet- and Fe-rich nature⁴. This heavy residue is prone to separation from its

overlying low-density granitoid batholith and eventual convective foundering into the mantle. A pulse of small-volume, high-potassium volcanism that erupted within a circular area about 200 km in diameter centred just south of Long Valley (Fig. 1a) apparently indicates both the locality and timing of the main removal event in the southern Sierra Nevada^{14,15}. This might represent only part of the area where the root was removed, as 3–4-Myr-ago volcanism extends much farther north and south¹⁶.

Receiver function seismology uses seismic waves produced by P- to S-wave mode conversions generated below seismic stations to image intracrustal and upper-mantle interfaces. Like reflection seismology, receiver functions are seismic traces that can be migrated to depth and geographically stacked to make pseudo-cross-sections of the subsurface in which the depths of continuous horizons, such as the Moho, can be identified and mapped. We stacked receiver functions calculated from teleseismic recordings in common conversion area bins (see, for example, refs 17–19). A crustal thickness map based on contouring the Moho P-to-s converted phase (Ps) reveals a complex pattern of thickness variations in the Sierra Nevada and surrounding regions (Fig. 1b). Beneath the northeastern corner of the study area, which includes the Big Pine volcanic field, the crustal thickness is about 36 km, 7–8 km thicker than the crust in Owens Valley farther south. The crust thickens westward, forming a crustal welt with a maximum thickness of 42 km beneath the Kings volcanic field. The Moho changes to a very different character south of the area of the high-potassium volcanism, where the crust in the Sierra Nevada is almost everywhere less than 36–37 km thick. Under the southern Owens Valley and adjacent ranges to the east, the Moho is relatively flat at ~30 km.

The pattern of crustal thickness variations determined from receiver functions agrees well with the results from seismic refraction studies²⁰. In particular, both indicate thicker crust (~40 km) beneath the Sierra Nevada north of about 36.5° latitude. The main difference between the two models that these methods produce is that the refraction model shows a bulge of thicker crust (~35 km) beneath the Owens Valley extending from south of Big Pine to about

36° latitude that is absent in the receiver function Moho-depth model (~30 km). Our crustal thicknesses are also in good agreement with an independent receiver function study done with the permanent stations in the Caltech network that overlap our study area²¹.

Three northeast–southwest receiver function cross-sections are shown in Fig. 2, with interpretations overlaid to highlight some interesting details of the crustal structure. The Moho is a large-amplitude, positive-polarity (red) arrival at depths between 30 and 42 km. In the southern cross-section (A–A') the Moho is a smooth interface, deepening gradually to the west, where the amplitude diminishes abruptly beneath the Great Valley. In the middle cross-section (B–B') the Moho arrival disappears farther east beneath the western edge of the range. In the northern cross-section (C–C') the Moho arrival is more complex, exhibiting an echelon offsets before disappearing even farther east beneath the western foothills. An absence of a clear wide-angle Moho reflection (PmP) from this portion of the crust was noted in the active source experiments, but it was attributed to noisy recording conditions in the Great Valley^{13,20}. In contrast, all the broadband stations were located on crystalline bedrock, and examination of data from the six stations sampling the region of absent Moho, some of which extend well into the western flank of the range, show that the disappearance is not due to interference from basin-generated noise.

The missing Moho in the western foothills (Fig. 1b) has two possible explanations. One scenario is that the shear velocity contrast at the Moho is significantly reduced by a localized zone of low S-wave velocity in the uppermost mantle, perhaps due to serpentinization of the mantle like that found in active forearc regions²². This is a plausible explanation, given that this region was within the forearc of a subduction zone until ~20 Myr ago. An alternative explanation is that small-scale topography on the Moho is scattering away the coherent Ps conversion, as well as the active

source PmP reflections. Later, we present synthetic modelling and additional independent evidence that supports this latter explanation.

Anisotropy in the lower crust

Another prominent feature in the cross-sections is a series of three en echelon negative-polarity arrivals (blue) observed in the middle to lower crust (at depths of ~20–30 km) throughout the study region (Fig. 2). This feature corresponds to the mid-crustal negative-polarity arrival (MCN) imaged in ref. 23 based on data from several small arrays deployed in an earlier study (MK, HM and DP00 in Fig. 1b). In the southern part of the study area, the top of this feature under Owens Valley is at a depth of ~20 km. Moving westward into the range, there appears to be a ~8–10 km en echelon step downward of the negative-polarity phase beneath the Sierra Nevada (A–A'). This 25-km-deep arrival underlies the entire high Sierra within the study area. Farther north (B–B'), the en echelon offset occurs beneath the eastern edge of the range. In the northern section where the crust thickens to a maximum of ~42 km, the thickening appears to occur in an en echelon fashion accompanied by another negative-polarity phase at ~35 km depth (C–C').

Analysis of directional variations in the negative-polarity arrival on the radial receiver function and its associated arrival on the tangential receiver function suggests the presence of an anisotropic layer at the base of the crust composed of an east-dipping fabric. The seismic anisotropy of this fabric is characterized by a slow direction perpendicular to an east or southeast-dipping plane, and equally fast directions in all orientations within that plane. One example of the azimuthal variations that results from the presence of anisotropy is displayed in the radial and tangential receiver functions for station JUN shown in Supplementary Information. We find that a planar fabric striking north–south to northwest–southeast and dipping at some amount greater than ~45° downward to the east or southeast

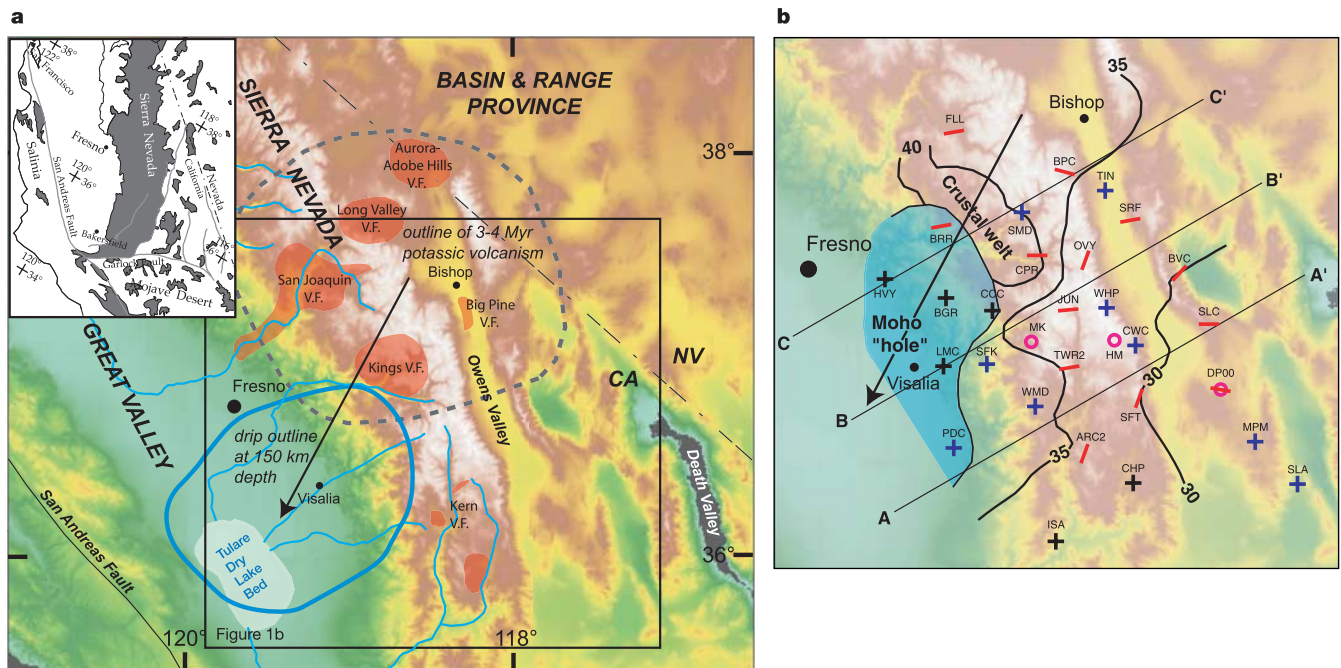


Figure 1 Study area and major results. **a**, Map of study area illustrating topography and drainage patterns, Cenozoic volcanic fields^{15,16,46}, outline of 3–4-Myr-ago potassic volcanism¹⁴ and outline of the mantle drip at 150-km depth¹³. Inset shows distribution of granitoid batholithic rocks in the Sierra Nevada, Mojave Desert and the Salinian terrane. **b**, Locations of broadband seismic stations used in this study are marked with symbols and station codes, indicating the presence and direction (short red dash) of lower-crustal anisotropy, absence of anisotropy (black 'plus' sign), or presence of some but differently

oriented anisotropy (blue 'plus sign'). Orientation of the dash is along the slow-wavespeed direction and perpendicular to the fabric orientation. Small open circles locate small arrays used in an earlier receiver function study²³. Thick black lines are contours of Moho depths (in km) estimated from stacked receiver functions. Thin black line with blue transparency outlines region with no Moho arrival in the stacked receiver functions that is interpreted as a Moho hole (see text for further explanation). Three cross-sections (A–A', B–B', C–C') are shown in Fig. 2.

provides the best fit to our data. Azimuthally varying patterns similar to those shown in Supplementary Information are found at most stations located in the Sierra Nevada and adjacent ranges across Owens Valley. Stations showing either different patterns or little evidence for crustal anisotropy are largely located within or near the edge of the Moho 'hole', near the eastern front of the Sierra Nevada, or south of latitude 36° N where the root was removed earlier (Fig. 1b).

Resolution tests

The common-conversion-point stacking technique employed here assumes that the P-to-S-converted phases are produced by laterally continuous horizontal structures, and does not account for focusing

or diffraction effects resulting from dipping or laterally varying interfaces. Images presented here display a dip on the Moho as well as negatively polarized arrivals that appear as a series of en echelon steps. We test the veracity of these images by determining whether or not we are able to resolve features with dips or steps with coarsely spaced stations. These tests are performed by computing synthetic receiver functions using a finite-difference algorithm (O. Boyd, personal communication) for various structures, and then processing the synthetics in the same way as the data. The station spacing and incidence angles of events in the synthetic tests are chosen to reflect those of the actual data. First, the presence of a structural cusp on the Moho was modelled to see how such a structure would appear in receiver function stacks (Fig. 3). The size of the cusp (50 km wide by 25 km deep) was made to be similar to the volume of crustal material entrained into the mantle by the 'drip' as it appears in the cross-sections and was based loosely on published numerical models. This is the feature responsible for creating the observed 'hole' in the Moho. In the cusp model, significantly diminished amplitude arrivals are observed centred over the cusp, demonstrating that a cusp-shaped feature can produce the observed Moho hole. No clear arrivals off the sides of the cusp were seen. The dipping edges of the cusp are too steep to be imaged here, but energy does arrive at the base of the cusp. The tests demonstrate that a V-shaped notch of crust ~50 km wide by ~25 km deep, cut into the mantle, is sufficient to make the Moho disappear in the receiver function stack. This is the basis for the V-shaped Moho holes interpreted in the cross-sections of Fig. 2. The western edge of the hole is poorly constrained owing to the absence of stations in the Great Valley. Second, we tested a series of models with a dipping Moho overlaid by an en echelon low-velocity zone with vertical offsets of varying magnitude (see Supplementary Information). We found that with our station spacing en echelon steps offset by at least 5 km can be recovered, while smaller steps can appear as a continuously dipping layer. Additionally, tests show that a continuously dipping low-velocity zone is not aliased into a series of steps.

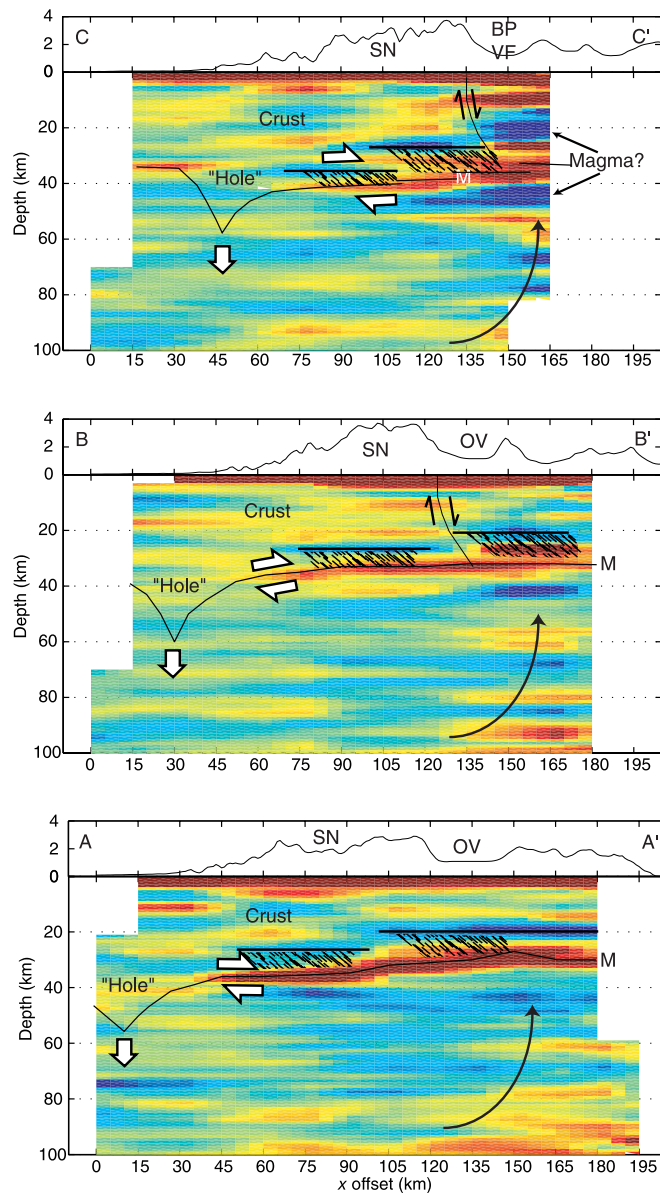


Figure 2 Cross-sections through the three-dimensional model of stacked receiver functions migrated into the depth domain and associated topography. Top panel, C–C'; middle, B–B'; bottom, A–A'; cross-sections are shown in Fig. 1b. Red areas represent large positive amplitudes (increase in wavespeed with depth), and blue areas represent negative amplitudes (decrease in wavespeed with depth). Hachure beneath prominent blue layers in crust represents east-dipping planar fabric producing seismic anisotropy. The V-shaped Moho holes are discussed in the text. SN, Sierra Nevada; BPFV, Big Pine volcanic field; OV, Owens Valley; M, Mono.

Alignment of crustal welt, Moho hole and mantle drip

The structural features and fabric of the crust that we have imaged do not correlate in any simple way with Sierran topography or geology. However, a revealing clue to the significance of these patterns is the alignment of major features along a southwest trend from near Bishop to Visalia (Fig. 1). Along this trend are the centre of the region of potassic volcanism, the crustal welt beneath the Kings volcanic field, the Moho hole beneath the adjacent foothills, the centre of the surface projection of the mantle drip and the Tulare dry lakebed. The final clue that provides a

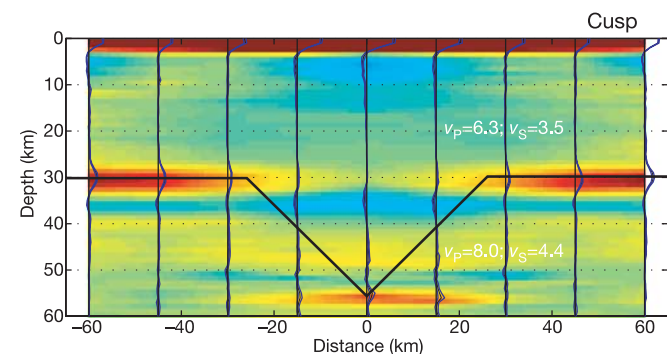


Figure 3 Synthetic stacked receiver function cross-section generated with a finite-difference wave-propagation technique for the seismic model shown beneath the image. The synthetic data were processed with station and bin spacings similar to those used with the southern Sierra Nevada data. v_p , P-wave velocity in km s^{-1} ; v_s , S-wave velocity in km s^{-1} .

connection among all these features is the recognition of a subsiding sub-basin in the Great Valley centred above the mantle anomaly²⁴. The locus of subsidence can be observed in the drainage patterns in the southern Sierra Nevada, where rivers discharging into the valley north of Fresno flow northward, while those within the circle of influence of the drip flow into the Tulare internal drainage basin (Fig. 1a). Ongoing work reconstructing sedimentation patterns suggests that the local sub-basin began forming at ~3–4 Myr ago and that it has migrated southwest to its current position²⁴. These observations can be connected to an active southwest-migrating convective instability. The alignment of features in the Sierra Nevada and the absence of similar features to the west suggest a strong asymmetry to the process. The localized crustal welt beneath the Kings volcanic field may reflect viscous drag at the base of the crust in the wake of southwest mantle motion (see, for example, refs 25–28). Numerical models of analogous convective instabilities^{29,30} show that at the point of downward detachment of the lithosphere, the lower crust will be entrained several tens of kilometres or more into the downward flow, providing an explanation for the V-shaped

Moho hole. The surface expression of the crustal foundering would be an elliptical zone of subsidence produced by viscous coupling between the downwelling drip and the overlying crust³¹.

We believe that the anisotropic fabrics observed near the crust–mantle boundary are associated with a shear zone between the crust and the foundering root. Well-developed shear zones generally have fabrics that are parallel to the shear zone, whereas fabrics or layering at an oblique angle to the shear plane are usually associated with the initial stages of shearing under brittle-ductile conditions³². The observed anisotropy could be due either to alignment of slow-axis minerals, such as mica, or to fluid- or melt-filled cracks in planes perpendicular to the axis direction. In both cases the planes containing the minerals or cracks dip east to northeast. The distinction between these two origins for the anisotropy is important, because they predict the opposite sense of shear with the same alignment (see Supplementary Information). The preferred interpretation is that the dipping fabric is related to fluid- or melt-filled fractures or veins formed during the initial stage of shearing. Cracks, fractures, or veins formed during shearing will

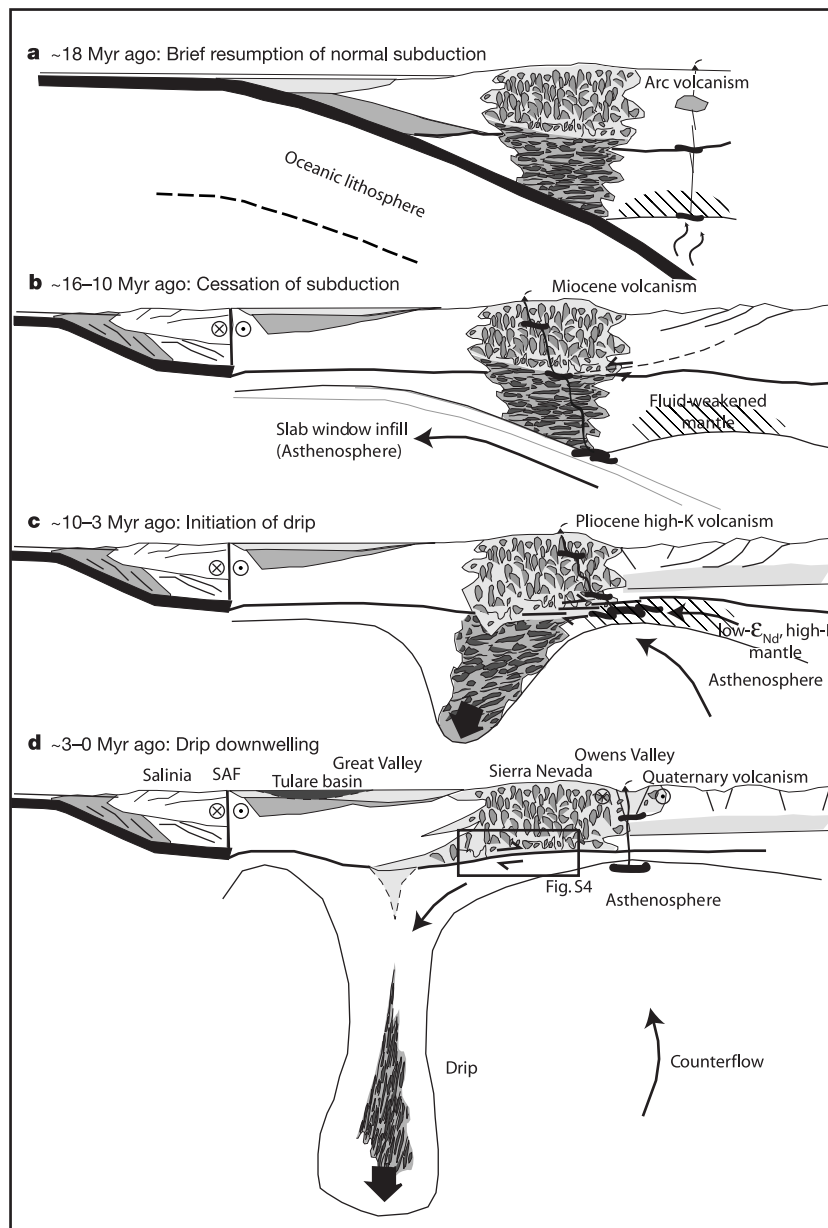


Figure 4 A sequential history of the foundering of the ultramafic root of the southern Sierra Nevada batholith. The proposed sequence is discussed in the text.

align in a direction antithetic to the shear direction; hence such features would be consistent with bottom-to-the-west shear. Laboratory experiments on feldspars at high temperatures and large shear strains showed melt segregated into melt-rich bands oriented obliquely to the shear plane and antithetic to the shear deformation³³. Fluids or melts are generally required to open and propagate fractures at these depths. (We know that at least some existed because even the limited Sierra Nevada volcanism³⁴ brought up xenoliths from such depths.) This interpretation requires high temperatures to trigger dehydration reactions or melting to induce fracturing. Although low temperatures are usually associated with convective instabilities³⁵, the formation of a shear zone between heterogeneous media can produce significant viscous heating³⁶. Even without shear heating, the rapid thinning of the lithosphere associated with asymmetric instabilities may be sufficient to locally raise mantle temperatures significantly. Quaternary volcanism, xenolith geothermometry and magnetotelluric measurements suggest the relatively recent attainment of high Moho temperatures (~1,000 °C), at least beneath Owens Valley^{7,8,37}. In an alternative interpretation that the anisotropy is due to oriented micas, the fabric is probably controlled by the development of an S-C fabric. In this case, the observed orientation of the anisotropy indicates top-to-the-west shear³², the opposite sense of the root moving westward into the drip (top-to-the-east sense of shear) but possibly consistent with an earlier phase of extension, suggesting a two-stage evolution involving a reversal in the sense of slip (see Supplementary Information).

Destabilization, detachment and sinking

Combining the new seismic results with the existing geologic constraints, we suggest the following sequence of events in the southern Sierra Nevada (Fig. 4). A dense root originated as an ultramafic phase of Sierran batholith formation during Mesozoic subduction. The Cretaceous granitic batholith and its garnet- and pyroxene-rich root formed a strong microplate under the influence of a cool geotherm that initiated during Laramide flat-slab subduction and is still reflected in modern heat flow (see, for example, ref. 38) and geothermometry (for example, refs 6, 39, 40). A number of factors could have played a role in destabilizing the root in the early Miocene. First, the volcanic arc returned to the northern Sierra (Fig. 4a), just within and north of the area pictured in Fig. 1 (ref. 41), terminating any unusually cool temperatures at the base of the continental lithosphere and possibly fluxing the Sierran lithosphere. Second, the Mendocino triple junction passed through this region between 10 and 20 Myr ago, exposing the Sierran lithosphere to the asthenosphere of the 'slab window' (Fig. 4b)⁴² and changing the basal stresses on the root¹¹. Third, extensional faults rooted into the Sierran crust developed starting at ~15 Myr ago (see, for example, ref. 34), weakening the top of the ultramafic root⁴³.

Although we have no direct information on the critical initial stages of the removal process, we suggest a history consistent with numerical models of lithospheric deformation in which the mechanical lithosphere (including the root) deforms by localized strain in the upper region in conjunction with Rayleigh–Taylor-type viscous deformation in the lower portion³⁰ (Fig. 4c). As the instability grew, a pronounced asymmetry in the foundering developed, resulting in a concentrated downwelling under the San Joaquin Valley and western foothills of the Sierra Nevada accompanied by a more widespread mantle upwelling under the western Basin and Range and easternmost Sierra (Fig. 4d). During this latter stage of development, the downwelling created a region of strong convergence in the mantle while the crust remained in a state of extension, suggesting decoupling (or a weak shear zone) between the crust and mantle except where the flow turns downward.

One explanation for the westward location of the downwelling is that the convective instability was initiated on the western edge of the batholith owing to compositional variations¹⁰, but a change in

the initiation location alone does not explain the asymmetric nature of the ensuing instability. Another explanation is that the instability was initially centred under the main crest of the Sierra but was displaced westward by asthenospheric flow related to the mantle wind⁴⁴ or to westward influx of asthenosphere into the slab window, a flow direction controlled by the shape and polarity of the palaeo-subduction zone^{45,46}. A third possibility, suggested by recent tomographic work⁴⁷, is that the garnet-rich material has descended roughly vertically but the removal has propagated from east to west, producing a dense, east- to southeast-dipping body connected at present to the crust at the Moho hole.

Numerical modelling of detachment of a lithospheric root that incorporates brittle crustal rheologies demonstrates that asymmetric formation of a convective instability is possible only if a prescribed dipping shear zone³⁰ or a laterally limited zone of weak brittle rheology is present²⁹. The hydrated lithosphere just east of the Sierra Nevada presumably established in the early Cenozoic above the subducting Farallon plate⁴⁸ is a likely location for such a laterally limited weak zone, especially given the initiation of extension in this region starting at ~15 Myr ago (see, for example, ref. 34). Westward motion of the detaching root would draw in weakened North American-affinity mantle from beneath the adjacent Basin and Range. Small-volume partial melting of this lithosphere mantle can reasonably explain the high-potassium, low- ϵ_{Nd} volcanism that occurred in the Sierra Nevada during the Pliocene¹⁵. Another important consequence of the asymmetric geometry of the removal process is the implication that the separation of the batholith from its root occurred along a concentrated zone of simple shear at the present-day Moho.

An important question remains unanswered: How much of the North American Cordilleran magmatic arc developed and then lost an ultramafic root? It is still debated whether the entire Sierra Nevada formed and lost its root^{16,44} or whether the removal is progressing northward and only the southern Sierra root is sinking, with the root remaining intact or in a nascent drip stage under the northern Sierra Nevada. The tectonic environment is obviously important in determining whether and when root removal occurs, but more documented examples are needed to clarify these relationships. Although not the focus of this Article, root foundering has important tectonic and geomorphic consequences—for example, collapse of the Salinian-Mojave block⁴⁹, uplift of the Sierra Nevada and its influence on adjacent ranges and faults¹⁶, and localized subsidence²⁴. Root removal is an important tectonic process with global implications, not only in terms of long-term crustal compositional evolution, but also in providing insights on lower-crustal deformation mechanisms, continental strength, and influence on regional tectonics. □

Received 16 February; accepted 12 July 2004; doi:10.1038/nature02847.

1. Ducea, M. N. The California arc: Thick granitic batholiths, eclogitic residues, lithospheric-scale thrusting, and magmatic flare-ups. *GSA Today* **11**, 4–10 (2001).
2. Kay, R. W. & Kay, S. M. Creation and destruction of lower continental crust. *Geol. Rundsch.* **80**, 259–278 (1991).
3. Kay, R. W. & Kay, S. M. Delamination and delamination magmatism. *Tectonophysics* **219**, 177–189 (1993).
4. Ducea, M. N. Constraints on the bulk composition and root foundering rates of continental arcs: A California arc perspective. *J. Geophys. Res.* **B 107**, doi:10.1029/2001JB000643 (2002).
5. Jull, M. & Kelemen, P. B. On the conditions for lower crustal convective instability. *J. Geophys. Res.* **106**, 6423–6446 (2001).
6. Ducea, M. N. & Saleeby, J. B. Buoyancy sources for a large, unrooted mountain range, the Sierra Nevada, California: Evidence from xenolith thermobarometry. *J. Geophys. Res.* **101**, 8229–8244 (1996).
7. Ducea, M. N. & Saleeby, J. B. A case for delamination of the deep batholithic crust beneath the Sierra Nevada, California. *Int. Geol. Rev.* **40**, 78–93 (1998).
8. Ducea, M. N. & Saleeby, J. B. The age and origin of a thick mafic-ultramafic keel from beneath the Sierra Nevada batholith. *Contrib. Mineral. Petrol.* **133**, 169–185 (1998).
9. Wernicke, B. *et al.* Origin of high mountains in the continents: The Southern Sierra Nevada. *Science* **271**, 190–193 (1996).
10. Saleeby, J., Ducea, M. & Clemens-Knott, D. Production and loss of high-density batholithic root—Sierra Nevada, California. *Tectonics* **22**, doi:10.1029/2002TC001374 (2003).
11. Zandt, G. & Carrigan, C. R. Small-scale convective instability and upper mantle viscosity under California. *Science* **261**, 460–463 (1993).
12. Jones, C. H., Kanamori, H. & Roecker, S. W. Missing roots and mantle "drips": Regional P_n and

- teleseismic arrival times in the southern Sierra Nevada and vicinity, California. *J. Geophys. Res.* **99**, 4567–4601 (1994).
13. Ruppert, S., Fliedner, M. & Zandt, G. Thin crust and active upper mantle beneath the Southern Sierra Nevada in the western United States. *Tectonophysics* **286**, 237–252 (1998).
 14. Manley, C. R., Glazner, A. F. & Farmer, G. L. Timing of volcanism in the Sierra Nevada of California: Evidence for Pliocene delamination of the batholithic root? *Geology* **28**, 811–814 (2000).
 15. Farmer, G. L., Glazner, A. F. & Manley, C. Did lithospheric delamination trigger late Cenozoic potassic volcanism in the Sierra Nevada, California? *Geol. Soc. Am. Bull.* **114**, 754–768 (2002).
 16. Jones, C. H., Farmer, G. L. & Unruh, J. Tectonics of Pliocene delamination of lithosphere of the Sierra Nevada, California. *Geol. Soc. Am. Bull.* (in the press).
 17. Dueker, K. G. & Sheehan, A. F. Mantle discontinuity structure from mid-point stacks of converted P to S waves across the Yellowstone hotspot track. *J. Geophys. Res.* **102**, 8313–8327 (1997).
 18. Kind, R. *et al.* Comprehensive seismic images of the crust and upper mantle beneath Tibet. *Science* **298**, 1219–1222 (2002).
 19. Gilbert, H. J., Sheehan, A. F., Dueker, K. G. & Molnar, P. Receiver functions in the western United States, with implications for upper mantle structure and dynamics. *J. Geophys. Res.* **B 108**, doi:10.1029/2001JB001194 (2003).
 20. Fliedner, M., Klemperer, S. L. & Christensen, N. I. Three-dimensional seismic model of the Sierra Nevada arc, California, and its implications for crustal and upper mantle composition. *J. Geophys. Res.* **105**, 10899–10921 (2000).
 21. Zhu, L. & Kanamori, H. Moho depth variation in southern California from teleseismic receiver functions. *J. Geophys. Res.* **105**, 2969–2980 (2000).
 22. Bostock, M. G., Hyndman, R. D., Rondenay, S. & Peacock, S. M. An inverted continental Moho and serpentinization of the forearc mantle. *Nature* **417**, 536–538 (2002).
 23. Jones, C. H. & Phinney, R. A. Seismic structure of the lithosphere from teleseismic converted arrivals observed at small arrays in the southern Sierra Nevada and vicinity, California. *J. Geophys. Res.* **103**, 10065–10090 (1998).
 24. Saleeby, J. & Foster, Z. Topographic response to mantle lithosphere removal in the southern Sierra Nevada region, California. *Geology* **37**, 245–248 (2004).
 25. Liu, M. & Shen, Y. Q. Sierra Nevada uplift: A ductile link to mantle upwelling under the basin and range province. *Geology* **26**, 299–302 (1998).
 26. Furlong, K. P. & Govers, R. Ephemeral crustal thickening at a triple junction: The Mendocino crustal conveyor. *Geology* **27**, 127–130 (1998).
 27. Neil, E. A. & Houseman, G. A. Rayleigh–Taylor instability of the upper mantle and its role in intraplate orogeny. *Geophys. J. Int.* **138**, 89–107 (1999).
 28. Houseman, G., Neil, E. A. & Kohler, M. D. Lithospheric instability beneath the Transverse Ranges of California. *J. Geophys. Res.* **105**, 16237–16250 (2000).
 29. Schott, B. & Schmeling, H. Delamination and detachment of a lithospheric root. *Tectonophysics* **296**, 225–247 (1998).
 30. Pysklywec, R. N., Beaumont, C. & Fullsack, P. Lithospheric deformation during the early stages of continental collision: Numerical experiments and comparison with South Island, New Zealand. *J. Geophys. Res.* **B 107**, doi:10.1029/2001JB000252 (2002).
 31. Bindschadler, D. L. & Parmentier, E. M. Mantle flow tectonics: The influence of a ductile lower crust and implications for the formation of topographic uplands on Venus. *J. Geophys. Res.* **95**, 21329–21344 (1990).
 32. Davis, G. H. & Reynolds, S. J. *Structural Geology of Rocks and Regions* 2nd edn (Wiley & Sons, New York, 1996).
 33. Zimmerman, M. E. & Kohlstedt, D. L. Melt segregation and LPO in anorthite-basalt deformed in torsion. *Eos* **84** (Fall Meet. Suppl.), S22E–06 (2003).
 34. Wernicke, B. P. in *The Geology of North America* Vol. G-3, *The Cordilleran Orogen: Conterminous US* (eds Burchfiel, B. C., Lipman, P. W. & Zoback, M. L.) 553–581 (Geological Society of America, Boulder, Colorado, 1992).
 35. Houseman, G. A. & Molnar, P. Gravitational (Rayleigh–Taylor) instability of a layer with non-linear viscosity and convective thinning of continental lithosphere. *J. Geophys. Res.* **128**, 125–150 (1997).
 36. Schott, B., Yuen, D. A. & Schmeling, H. Viscous heating in heterogeneous media as applied to the thermal interaction between crust and mantle. *Geophys. Res. Lett.* **26**, 513–516 (1999).
 37. Park, S. K., Hirasuna, B., Jiracek, G. R. & Kinn, C. L. Magnetotelluric evidence of lithospheric mantle thinning beneath the southern Sierra Nevada. *J. Geophys. Res.* **101**, 16241–16255 (1996).
 38. Saltus, R. W. & Lachenbruch, A. H. Thermal evolution of the Sierra Nevada: Tectonic implications of new heat flow data. *Tectonics* **10**, 325–344 (1991).
 39. Dumitru, T. A. Subnormal Cenozoic geothermal gradients in the extinct Sierra Nevada magmatic arc: Consequences of Laramide and post-Laramide shallow-angle subduction. *J. Geophys. Res.* **95**, 4925–4942 (1990).
 40. House, M. A., Farley, K. F., Wernicke, B. P. & Dumitru, T. A. Cenozoic thermal evolution of the central Sierra Nevada from (U–Th)/He thermochronology. *Earth Planet. Sci. Lett.* **151**, 167–179 (1997).
 41. Dickinson, W. R. The Basin and Range Province as a composite extensional domain. *Int. Geol. Rev.* **44**, 1–38 (2002).
 42. Atwater, T. & Stock, J. Pacific–North America plate tectonics of the Neogene southwestern United States: An update. *Int. Geol. Rev.* **40**, 375–402 (1998).
 43. Molnar, P. & Jones, C. H. A test of laboratory-based rheological parameters of olivine from an analysis of late Cenozoic convective removal of mantle lithosphere beneath the Sierra Nevada, California, USA. *Geophys. J. Int.* **156**(3), 555–564 (2004).
 44. Zandt, G. The southern Sierra Nevada drip and the mantle wind direction beneath the southwestern United States. *Int. Geol. Rev.* **45**, 213–224 (2003).
 45. Furlong, K. P., Lock, J., Guzowski, C., Whitlock, J. & Benz, H. in *The Lithosphere of Western North America and its Geophysical Characterization, The George A. Thompson Volume* (eds Klemperer, S. L. & Ernst, W. G.) 92–104 (International Book Series, Vol. 7, Bellwether Publishing/Geological Society of America, Boulder, Colorado, 2003).
 46. Hartog, R. & Schwartz, S. Y. Subduction induced strain in the upper mantle east of the Mendocino triple junction, California. *J. Geophys. Res.* **105**, 7909–7930 (2000).
 47. Boyd, O. S., Jones, C. H. & Sheehan, A. F. Foundering lithosphere imaged beneath the southern Sierra Nevada, California, USA. *Science* **305**, 660–662 (2004).
 48. Lange, R. A., Carmichael, I. S. E. & Renne, P. R. Potassic volcanism near the Mono basin, California: Evidence for high water and oxygen fugacities inherited from subduction. *Geology* **21**, 949–952 (1993).
 49. Saleeby, J. B. Segmentation of the Laramide slab—Evidence from the southern Sierra Nevada region. *Geol. Soc. Am. Bull.* **115**, 655–668 (2003).

Supplementary Information accompanies the paper on www.nature.com/nature.

Acknowledgements G.Z. thanks G. Gehrels, P. Kapp and B. Hacker for comments on preliminary interpretations and manuscripts.

Authors' contributions G.Z., H.G., T.J.O. and C.H.J. cooperated on the seismology analysis and interpretation. M.D. and J.S. provided the geologic and tectonic context. C.H.J. led the PASSCAL deployment to collect the data. G.Z. wrote the Article with contributions from all the authors.

Competing interests statement The authors declare that they have no competing financial interests.

Correspondence and requests for materials should be addressed to G.Z. (zandt@geo.arizona.edu).